Electronic Supplementary Material (ESI) for Physical Chemistry Chemical Physics.

SUPPLEMENTARY INFORMATION

Dynamic micellar oligomers of amyloid beta peptides play a crucial role in their aggregation mechanisms

Bertrand Morel[1*], Maria Paz Carrasco[2], Samuel Jurado[1], Carmen Marco[2] and Francisco Conejero-Lara[1*]

[1] Departamento de Química Física e Instituto de Biotecnología, Facultad de Ciencias, Universidad de Granada, 18071 Granada, Spain

[2] Departamento de Bioquímica y Biología Molecular I, Facultad de Ciencias, Universidad de Granada, 18071 Granada, Spain

***Corresponding author**:

B. Morel; tel. +34 958 240437; e-mail: bmorel@ugr.es.

F. Conejero-Lara; tel. +34 958 242371; e-mail: conejero@ugr.es.

Supplementary Text: Mass-action model for Aβ micelle formation

Our experimental data suggest that disaggregated Aβ undergoes a micellization-like self-association equilibrium. The simplest model for micelle formation is the so-called mass action model [1, 2] where the formation of a micellar oligomer O_m from m monomers is considered fully cooperative:

$$mM \rightleftarrows O_m$$

The micellization equilibrium constant is:

$$K_m = \frac{[O_m]}{[M]^m} = \exp\left(-\frac{m\Delta G_m^o}{RT}\right)$$

where ΔG_m^o is the standard Gibbs energy of micelle formation. We ignore here the effect of non-ideality of the solutions and counter ion binding, which can be incorporated into the ΔG_m^o value, as a function of environmental variables [3]. For sufficiently high m, the critical micelle concentration (*CMC*) is given by [2]:

$$CMC \approx \left(\frac{1}{K_m}\right)^{1/m} \qquad (1)$$

A more accurate *CMC* is however given by:

$$CMC = \left(\frac{(m-2)}{m^2 K_m (2m-1)}\right)^{1/(m-1)} + mK_m \left(\frac{(m-2)}{m^2 K_m (2m-1)}\right)^{m/(m-1)} \qquad (2)$$

In absence of other types of aggregates, for instance at time zero in an aggregation kinetics from fully disaggregated Aβ, the total mass concentration of peptide:

$$C = [M] + m[O_m] = [M] + mK_m[M]^m \qquad (3)$$

This equation can be solved to obtain the free M concentration for each total peptide concentration given a micelle size and a micellization constant. From *[M]* we can calculate the mass concentration of micellar oligomers:

$$C_O = m[O_m] = mK_m[M]^m \qquad (4)$$

These equations can be used to fit the bis-ANS fluorescence and the light scattering intensities as a function of the total peptide concentration for LMW-Aβ. The bis-ANS fluorescence intensity is given by:

$$S^{ANS} = S_0 + F_M^{ANS}[M] + F_O^{ANS} C_O \qquad (5)$$

where the *F* parameters are the specific fluorescence of the *M* and the *O* aggregates due to bis-ANS binding. Similarly, the scattering intensity of a monomer-aggregate mixture is:

$$S^{Sc} = S_0 + K[M] + KmC_O \qquad (6)$$

where S_0 is a background scattering intensity and *K* is an optical constant. The scattering intensity of the Aβ peptide in the micelles is proportional to their size *m*.

Interpretation of the initial aggregation rates

Above the *CMC* the initial slopes of the aggregation kinetics observed by bis-ANS and ThT fluorescence increase linearly with concentration. This indicates that the kinetics approach a first-order regime. Below the *CMC* the double-log plots appear to approach to second-order regime. Then, we can assume that Aβ nucleation can take place by two parallel competing processes, depending on the micellization pre-equilibrium. At concentrations below the *CMC*, bimolecular primary nucleation dominates [4], whereas above the *CMC* Aβ nuclei are mainly formed within the micellar oligomers [5]. The initial rate of formation of amyloid nuclei, *A*, is therefore:

$$r_0 = \left(\frac{dC_A}{dt}\right)_{t\to 0} = n_c k_{nO} C_O + 2k_{nM}[M]^2 \qquad (7)$$

where k_{nO} and k_{nM} are the first-order and second-order rate constants for each primary nucleation process. n_c is size of the Aβ nuclei formed within the micelles.

Since the *O* species may also show binding to the fluorescence dyes, the slopes of the kinetics near and above the *CMC* can be affected not only by the rate of formation of the *A* nuclei but also by the rate of disappearance of the *O* oligomers due to their reversible dissociation as the concentration of non-amyloid Aβ is being depleted. The rate of change of the *O* species is given by:

$$\frac{dC_O}{dt} = -\frac{dC_A}{dt} - \frac{d[M]}{dt} \qquad (8)$$

During aggregation, equation (3) is modified by the appearance of *A* species as:

$$mK_m[M]^m + [M] = C - C_A \qquad (9)$$

And taking the time derivative and solving for the rate of change of [M]:

$$\frac{d[M]}{dt} = -\frac{1}{1 + m^2 K_m [M]^{m-1}} \frac{dC_A}{dt} = -G([M])\frac{dC_A}{dt} \qquad (10)$$

where G([M]) is a function of [M] and the parameters of the micellization equilibrium. Using the equations described above, the initial slope for an aggregation kinetics monitored by fluorescence is:

$$r_0^{Fl} = F_A \frac{dC_A}{dt} + F_O \frac{dC_O}{dt} = \left(F_A - F_O\right)\frac{dC_A}{dt} + F_O G\left(\left[M\right]\right)\frac{dC_A}{dt}$$
$$= \left[\Delta F + F_O G\left(\left[M\right]\right)\right]\left(k_{nO} C_O + k_{nM}\left[M\right]^2\right) \qquad (11)$$

And in double-log plot:

$$\log\left(r_0^{Fl}\right) = \log\left[\Delta F + F_O G\left(\left[M\right]\right)\right] + \log\left(k_{nO} C_O + k_{nM}\left[M\right]^2\right) \qquad (12)$$

In these equations ΔF is the specific fluorescence change of Aβ due to its conversion to aggregation nuclei. In principle, this set of equations can be used to fit the dependences of the initial rates of aggregation with the total concentration of Aβ peptide, using k_{n0}, k_{nM} and ΔF as fitting parameters. The parameters of the micellization pre-equilibrium can be fixed using those determined independently from the scattering measurements (Figure S2a) and the F_0 value for the bis-ANS kinetics can be also obtained from direct bis-ANS measurements of disaggregated Aβ (Figure 2b) and fixed in the fittings. F_0 was fixed to zero for the ThT kinetics, since the micellar oligomers do not bind ThT significantly. However, there is a strong interdependency between ΔF and the two rate constants. Because $F_0 \cdot G([M])$ is always much lower than ΔF, the first term on the right-hand side of Equation 12 is approximately constant, so that ΔF cannot be determined from the fittings. Accordingly, we fixed ΔF using a sufficiently high value (10^7) and fitted the double log plots to obtain relative k_{n0} and k_{nM} values.

Figure S1. Purification and size characterization of LMW-Aβ40. (a) Typical size-exclusion chromatography elution for disaggregated Aβ40. The inset shows an expansion of the main elution peak. (b) Particle size distributions obtained by DLS for the different fractions collected along the main elution peak as shown in (a).

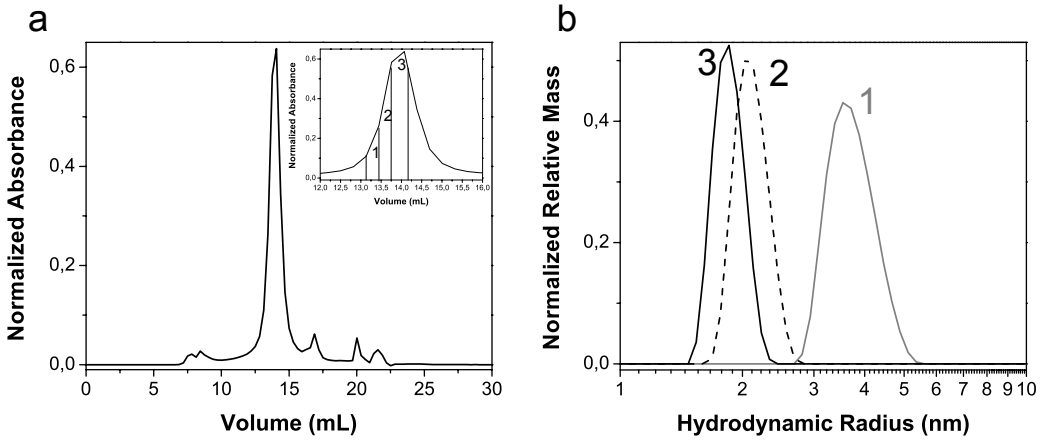

Figure S2. Determination of the critical micelle concentrations of LMW-Aβ40 and LMW-Aβ42 using pyrene fluorescence (a-b). Ratio of vibronic band intensities I_{III}/I_I as a function of peptide concentration. The symbols correspond to the experimental points and the lines represent the best fits according to a Boltzman sigmoid.

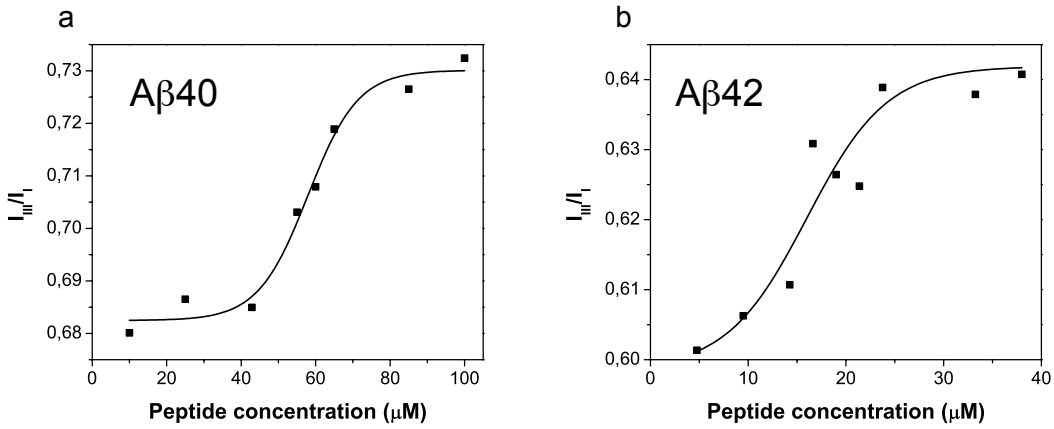

Figure S3. Characterization of the micellization equilibrium of LMW-Aβ40 and LMW-Aβ42 using the mass-action model equations, as described in the Supplementary Text. (a) Fittings of the scattering intensity (a) and Bis-ANS fluorescence intensity (b) as function of the peptide concentration.

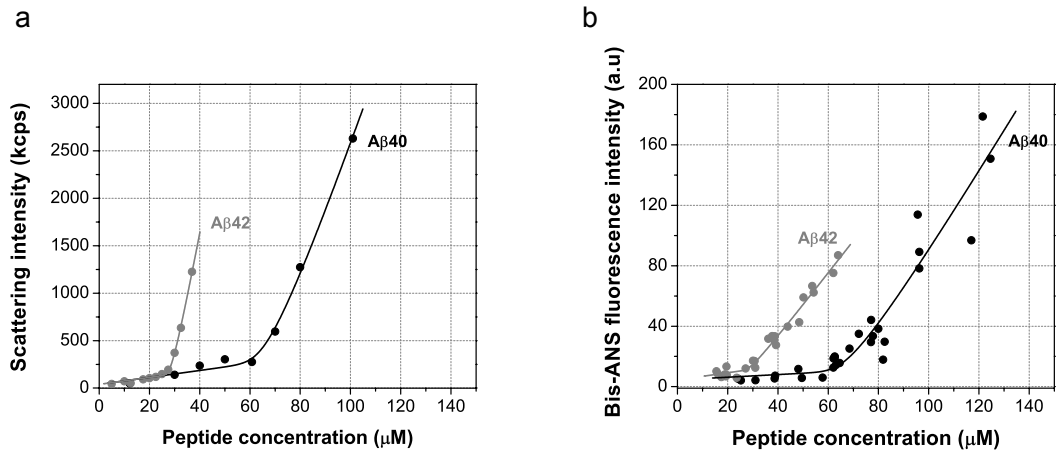

Table S1. Secondary structure analysis of LMW-Aβ40 and LMW-Aβ42 derived from the deconvolution of the amide I band of the FTIR spectra obtained at t0 and after 400 minutes of incubation at 37°C.

	LMW-Aβ40		**LMW-Aβ42**	
	t0	t=400 min	t0	t=400 min
Random coil (%) [a]	56.1	46.5	27.9	24.2
β-sheet (%) [b]	27.5	38.8	41.6	51.8
β-turns (%) [c]	16.5	14.7	30.4	24.0
Intermolecular β-sheet (%) [d]	27.5	38.8	37.5	48.6

Table S2. Secondary structure analysis of the oligomers derived from the deconvolution of the amide I regions of the FTIR spectra obtained at t0 and after 400 minutes of incubation at 37°C.

	Aβ40-OA		**Aβ42-OA**		**HMW-Aβ42**	
	t0	t=400 min	t0	t=400 min	t0	t=400 min
Random coil (%) [a]	15.9	-	47.3	35.7	19.3	22.9
β-sheet (%) [b]	44.0	72.9	35.4	39.5	54.5	55.9
β-turns (%) [c]	40.1	27.1	17.3	24.8	26.2	21.2
Intermolecular β-sheet (%) [d]	37.3	46.7	11.3	21.6	14.3	50.3

*Characteristic amide I wavenumbers obtained from [6].

[a]: Random coil : 1645 cm^{-1} – 1655 cm^{-1}
[b]: β-sheet : 1620 cm^{-1} - 1640 cm^{-1} ; 1670 cm^{-1} - 1695 cm^{-1}
[c]: β-turns : 1685 cm^{-1} - 1655 cm^{-1}
[d]: Intermolecular β-sheet : 1627 cm^{-1} - 1615 cm^{-1}

References

1. P. Debye, *J. Phys. Colloid Chem.*, 1949, **53**, 1-8.
2. H. Wennerstrom and B. Lindman, *Physics Reports*, 1979, **52**, 1-86.
3. C. Tanford, *Proc. Natl. Acad. Sci. USA*, 1974, **71**, 1811-1815.
4. T. P. Knowles, C. A. Waudby, G. L. Devlin, S. I. Cohen, A. Aguzzi, M. Vendruscolo, E. M. Terentjev, M. E. Welland and C. M. Dobson, *Science*, 2009, **326**, 1533-1537.
5. A. Lomakin, D. B. Teplow, D. A. Kirschner and G. B. Benedek, *Proc. Natl. Acad. Sci. USA*, 1997, **94**, 7942-7947.
6. S. A. Tatulian, *Methods Mol. Biol.*, 2013, **974**, 177-218.